Workshop on Visualisation in Environmental Sciences (EnvirVis) (2017)
R. Bujack and A. Middel and K. Rink and D. Zeckzer (Editors)

An Interactive Web-based Doppler Wind Lidar Visualisation System

N. Tan Jerome[1] S. Chilingaryan[1] A. Kopmann[1] A. Wieser[2]

[1]Institute for Data Processing and Electronics, Karlsruhe Institute of Technology, Germany
[2]Institute of Meteorology and Climate Research, Karlsruhe Institute of Technology, Germany

Abstract

With Doppler wind lidar producing significant amounts of data, providing means to extract relevant information from the data that describes atmospheric phenomena such as rain and low-level clouds is of vital importance. However, a Doppler wind lidar with a 10 Hz *sampling rate produces large-scale of data at approximately ten million data items per day; therefore, introducing challenges in perceptual and interactive scalability. We present an interactive web-based visualisation system that provides summary displays of the heterogeneous lidar data. Our system applies the client-server paradigm, where our server extracts information and encodes primary lidar attributes into image's colour channels. Then, we load these encoded images and show lidar data in multiple forms at the client-side. In contrast to script-based tools such as Matlab and Ferret, our system allows researchers to begin analysing the extensive data using a more top-down methodological approach. In particular, we implemented features like zooming, multivariate filtering, and hourly variance heat map, in which GPU shaders filter data according to specific attributes. With the encoded images readily stored at the server, researchers can browse through the vast amounts of data interactively.*

Categories and Subject Descriptors (according to ACM CCS): I.3.3 [Computer Graphics]: Picture/Image Generation—Multivariate Encoded Image I.3.8 [Computer Graphics]: Applications—Doppler Wind Lidar Visualization

1. Introduction

In climate research, a major visualisation task is exploring unknown patterns and structures [SN14]. By using Doppler wind lidar, researchers can gain insights into daily phenomena such as rain, updraft, downdraft, fast moving low clouds and nocturnal low-clouds [AKG17, SFK13]. We can identify these events from the lidar's primary attributes: wind velocity, backscattering coefficient, and signal-noise-ratio. Also, we orchestrate the lidar's illumination direction in azimuth and elevation angles for more information:

- Vertical Stare: a fixed arbitrary azimuth angle and a fixed elevation angle at 90°.
- Plan Position Indicator (PPI): varying azimuth and fixed arbitrary elevation angles.
- Range Height Indicator (RHI): fixed arbitrary azimuth and varying elevation angles.

Despite various setups and attributes of lidar data, they are stored together in one repository which complicates the overall data processing and visualisation. These data with different configurations must be preprocessed and presented in a variety of standard visualisations [NSBW08]. Moreover, a Doppler wind lidar system with 10 Hz sampling rate produces large-scale of data at approximately 10 million of data items per day; therefore, introducing challenges in perceptual and interactive scalability [LJH13]. Based on the survey by Tominski et al. [TDN11], researchers often use script-based tools such as Matlab and Ferret to process and produce static images for visual inspection. However, these traditional tools were not suitable for the scale and heterogeneity of such lidar data [Mad12, CDD*09, FH09].

Our goal is to provide an interactive web-based lidar visualisation for better data exploration and analysis. Our system applies the client-server paradigm, with our server extracting information and encoding primary lidar attributes into image's colour channels. At the client-side, we load these encoded images and show lidar data in multiple forms. In contrast to having many static images, our system allows researchers to begin analysing the extensive data using a more top-down methodological approach by introducing a daily view and an hourly view. In particular, we implemented features like zooming, multivariate filtering, and hourly variance heat map, in which data can be filtered according to certain attributes interactively. In this paper, we contribute methods to enable interactive viewing and analysis on large amounts of complex lidar data. Our contributions are:

- Data reduction and aggregation on large-scale heterogeneous lidar data.
- Encoding primary lidar attributes into image's colour channels for client-side multivariate visualisation.
- Storing all the encoded images at the server for high-speed data browsing.

DOI: 10.2312/envirvis.20171097

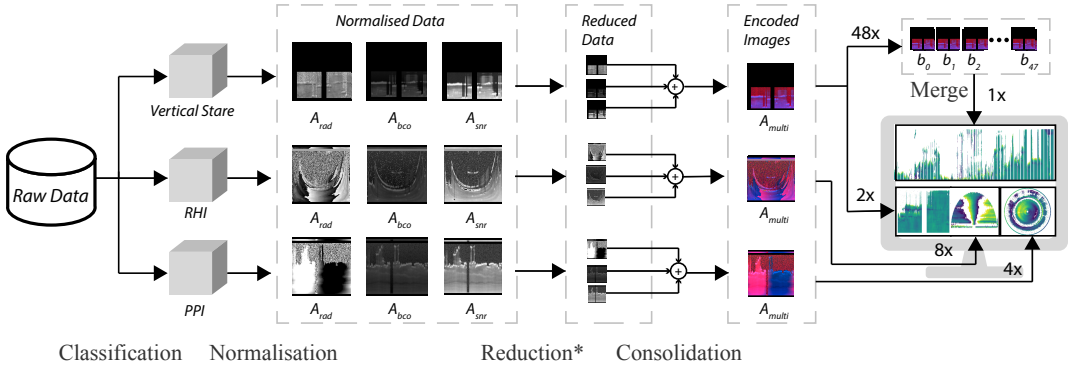

Figure 1: *The data preprocessing component in our system, which comprises of data classification, data normalisation, data reduction, and data consolidation stages. A_{rad}, A_{bco}, and A_{snr} denote grey images for the wind velocity, the backscattering coefficient, and the signal-noise-ratio attributes, respectively. * We perform data reduction only when the total size of grey images exceeds* 1 MB.

- Improving performance in client visualisation using GPU shaders.
- Performing multivariate filtering method, zooming, and hourly variance heat map to detect, validate, and discover data patterns.

2. Related Work

As the Doppler wind lidar system often comes with a dedicated user interface for online monitoring, there is no demand to have a separate offline visualisation system [HH05, TLCS12]. Furthermore, standard displays for the Doppler wind lidar are readily producible in offline mode using any conventional graphics display packages. Hofmeister et al. [HBF*15] evaluated their Doppler wind lidar using a custom LabVIEW display tool. Prasad et al. [PSV*15] also evaluated their lidar system using a custom display tool called Windimager. However, they often use the script-based approach such as Matlab [MAT10] and Ferret [HHO*96] for offline data processing and analysis [TDN11]; thus, suffering in performance due to the data size and complexity [Mad12, CDD*09, FH09].

Although most lidar visualisation systems are attached to the hardware, there are also standalone systems available. Wang et al. [WHW13] presented a display system that integrates Google Maps with a microscale meteorological model to improve their overall system's functionality. They extended their system to visualise Doppler wind lidar data as well. Cherukuru and Calhoun [CC16] developed a smartphone application to perform lidar visualisation in augmented reality. Their work opens up visualisation opportunity in lidar visualisation and spun idea for virtual reality implementation [BBH*17]. These applications emphasised on overlaying lidar data on a terrain or a 3D environment to increase spatial awareness. Rather than coupling with the lidar hardware, their systems rely instead on external resources, i.e. the system by Wang et al. [WHW13] requires an interface to Google services and the smartphone application by Cherukuru and Calhoun [CC16] needs a virtual reality goggle.

Our work aims to provide a visualisation platform with better performance that supports online and offline measurement phases. Thus, we developed a web-based tool that is not restricted by any external dependencies and our system stores cache data (encoded images) at the server for high-speed data browsing.

3. Use Case

We use the Doppler wind lidar data collected over the course of 2 months from the KITcube mobile observation platform [KAW*13], which the platform operates in conjunction with the Dynamics-aerosol-chemistry-cloud interactions in West Africa (DACCIWA) Campaign [KCC*15]. During each 30 minutes interval throughout the campaign, the Doppler wind lidar performed two PPI scans, four RHI scans, and followed by a vertical stare sweep.

4. System Design

An efficient web-based visual analysis system must address the network latency and the interactive client performance [TJCS*17]. Thus, our visualisation system is composed of client-server components. At the server, we perform data preprocessing by reducing the data size and later transforming them into images encoded by primary lidar attributes.

At the client, we load these encoded images into the GPU texture memory through WebGL [Khr11]. Depending on the type of lidar scans, each view in summary visualisations is mapped to its intended geometry accordingly, e.g. vertical stare to a rectangle, PPI to a circle, and RHI to a segment (Figure 1). While performing data manipulation in the GPU shader, our client views can update its content interactively. We chose GPU shaders mainly to improve the performance of our client visualisation.

4.1. Data Preprocessing

Figure 1 shows the server component of our system. The main idea is to process heterogeneous lidar data and to reduce the size for a better network latency. After each completed lidar scan combination, collected data are packed and sent to the central server for data archival and processing. Upon receiving the incoming data packet, our system triggers the data preprocessing immediately to generate and store encoded images at the server. We follow the approach

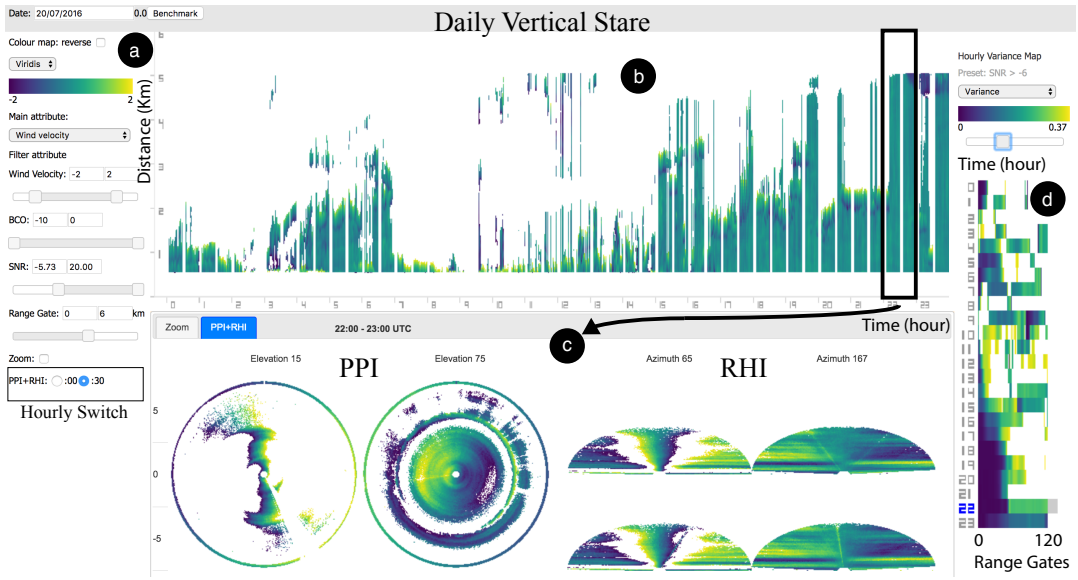

Figure 2: *A screenshot of our client web-based visualisation component, which comprises of four sections. They are (a) parameter selection to perform multivariate filtering method, (b) daily overview of the vertical stare plot, (c) hourly vertical stare, PPI, and RHI schemes, and (d) hourly variance heat map. Using the hourly switch radio buttons, we enable selection between the first or second half 30 minutes of the chosen hour. Here, we had chosen blue-green-yellow colour map as an example, and users have the opportunity to select another variant of colour maps.*

proposed by Liu et al. [LJH13], where cache data (encoded images) are precomputed and stored for a seamless user experience in data transitions. In the context of our summary visualisations, we merge 48 vertical stare data to form the final image in the daily view; and, we show two vertical stare, four PPI, and eight RHI plots in the hourly view (Figure 2).

Initially, we classify lidar data according to its azimuth and elevation angles. This classification results in three groups of data set, namely vertical stare, PPI, and RHI. Since the sampling time of the data may vary indefinitely, we normalise the time series data using linear interpolation. For each data set, we prepare three grey images based on lidar's primary attributes: wind velocity (A_{rad}), the backscattering coefficient (A_{bco}), and the signal-noise-ratio (A_{snr}). We map the image's x-axis to time (second) and y-axis to the laser distance of lidar (metre). The resulting grey image has 1800 pixels width and 1000 pixels height, which corresponds to 1800 s in x-domain and 10 000 m in y-domain. We chose 10 000 m to cover the longest laser distance within all lidar scanning setups, which means one pixel corresponds to 10 m on the y-axis.

To address the network latency, we reduce the size of grey images down for a better bandwidth transmission. According to the work by Tan Jerome et al. [TJCS*17], a data size of lower than 2 MB ensures an interactive response on a Wifi network preset (30 Mb/s). In the data reduction step, we perform image downscaling on whichever set of grey images that have a total size exceeding 1 MB. In our use case, the 30-minutes vertical stare, PPI, and RHI plots are less than our defined threshold. However, the combination of 48 vertical stare plots that forms a daily plot has a size exceeding the threshold; therefore, we downscale these images in x-direction using the Lanczos filter from ImageMagick. Depending on the different client performances, we can adapt the downscale factor for better performance.

Rather than transferring these grey images directly to the client, we combine each set of grey images consisting of its corresponding lidar primary attributes to minimise the number of images for the GPU texture memory. Here, we address the restriction presented by the client regarding texture unit, in which texture unit defines the number of texture image renderable at a time. From the precomputed grey images, we create a multivariate image by encoding the wind velocity attribute into the red colour channel, the backscattering coefficient attribute into the green colour channel, and the signal-noise-ratio attribute into the blue colour channel.

4.1.1. Variance Heat Map

In addition to the standard lidar displays, our heat map widget provides researchers insights into the wind velocity variation of hourly vertical stare images (Figure 2d). We had chosen the heat map matrix because we can preserve the spatial information of the data attribute with respect to time and distance. Within each hourly vertical stare image, the distance along the lidar's laser consists of smaller segments, namely range gates. In our use case, we have a total of 120 range gates based on the lidar setup. We summarise wind velocity attributes along each range gate across the one hour image into one representative variance; thus, resulting in a heat map matrix. The vertical axis corresponds to hours from top to bottom, and the horizontal axis corresponds to the range gate distance from

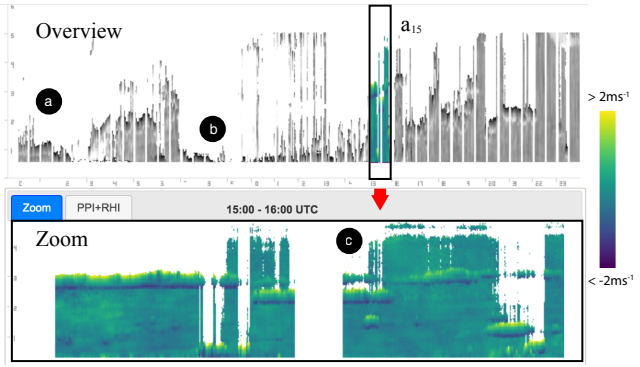

Figure 3: *A zooming interface with two views: A daily view (overview) and an hourly view (zoom). The daily view consists of 24 equally divided hourly segments, with the selected segment, a_{15}, depicting the 15th hour. (a) suggests the formation of nocturnal low-level clouds [AKG17, SFK13], (b) indicates a rain event, and (c) suggests a fast moving low clouds.*

left to right. We colour each unit using the same colour map used throughout our system. To assign a variance interval, we defined our lower and upper bounds based on the Von Szokefalvi Nagy inequality (lower bound) and the Bhatia-Davis inequality (upper bound) [SGK10].

4.2. Data Visualisation

We create our client data visualisation in Javascript, which we based on the ThreeJS library [Cab11] that utilises the WebGL. The Javascript language offers platform independence, and it is compatible with every major client browser [MKRE16]. Figure 2 shows our visualisation system, which emphasises on the daily overview and the hourly view. Due to the limited screen viewport, it is inevitable that visualising large amounts of temporal data results in lost of details. In response, numerous works emphasise in multi-focus interaction [EHRF08,ZCPB11]. Among these techniques, we implemented a zooming interface, which uses a temporal separation between the views [CKB09]. The daily view consists of 24 equally divided hourly segments, $(a_0 \cdots a_{23})$. By hovering over a segment, we provide a more detailed hourly view. The combination of the daily view and the hourly view allows researchers to detect atmospheric events, such as nocturnal low-level clouds, rain event, updrafts, and downdrafts (Figure 3).

A most demanded feature in data browsing is the ability to inspect multiple attributes interactively [RTL*16]. Here, we can show or filter out data based on the wind velocity, the backscattering coefficient, and the signal-noise-ratio thresholds. To investigate the vertical wind velocity profile, researchers often start with a range criteria between $-2\,\mathrm{m\,s^{-1}}$ and $2\,\mathrm{m\,s^{-1}}$. Alternatively, having the possibility to adjust the range criteria to focus on any arbitrary wind velocity range is beneficial. Moreover, researchers can filter out data by changing the value criteria of other attributes. These adjusted criteria update and synchronize data content across all viewports interactively.

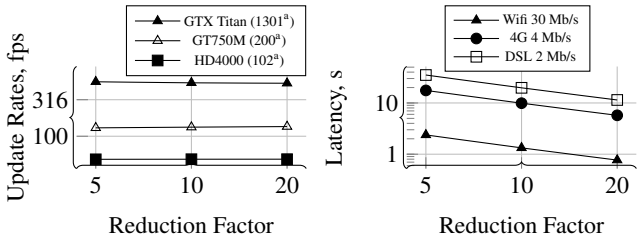

Figure 4: *Latency and update rates of reduced data by a factor of 5, 10, and 20 on multiple network conditions and client hardware. [a] refers to frame rates metric of the GPU taken from the WAVE framework (higher the better) [TJCS*17].*

5. Evaluation

The overall performance of our system is evaluated based on the responsiveness of the client-side rendering and the latency between server-client interaction. Thus, we performed tests to measure the network latency and the update rates for various data sizes. For this evaluation, we evaluated data reduced by a factor of 5 (7.2 MB), a factor of 10 (3.4 MB), and a factor of 20 (1.3 MB). Using these data, we performed a series of multivariate filterings on a MacbookPro (GT750M), a desktop with integrated graphic card (HD4000), and a high-performance desktop (GTX Titan). Here, we wrote a Javascript code that updates the filtering slider progressively for each attribute and recorded the average update rates. Figure 4 (left) shows that update rates are not affected by the data size, but rather by the hardware quality. On the other hand, the data size dictates the performance of the network latency, in which Figure 4 (right) shows an improvement in latency the smaller the data size gets. Ideally, setting up the system in a local area network will improve the latency significantly.

Our results showed the effectiveness of our system as our update rates are higher than 30 fps [CC06]. Even the desktop with only an integrated graphic card (HD4000) scored average update rates of 48 fps. Although we reduced the daily vertical stare to fit the viewport, we integrated a variance heat map to provide insights on the hourly wind velocity variation. Moreover, our client system provides more details with the hourly zoom view as shown in Figure 3. In Figure 2d, the researcher can identify whether there is high wind velocity variation at the lower or upper range gates. Also, we could interpret that rain event took place between 0800 to 1400 hours based on the missing elements.

6. Conclusion

We present an interactive web-based visualisation system for Doppler wind lidar to address challenges in data exploration and data analysis. Our system performs data reduction and aggregation during online measurement phase, and store precomputed encoded images at the server. Using these encoded images, we show standard lidar displays by using GPU shaders, thus resulting in a highly interactive system. With encoded images readily stored at the server, researchers can browse through the vast amounts of data interactively.

References

[AKG17] ADLER B., KALTHOFF N., GANTNER L.: Nocturnal low-level clouds over southern west africa analysed using high-resolution simulations. *Atmospheric Chemistry and Physics 17* (2017), 899–910. doi:10.5194/acp-17-899-2017. 1, 4

[BBH*17] BERGMANN T., BALZER M., HOPP T., VAN DE KAMP T., KOPMANN A., TAN JEROME N., ZAPF M.: Inspiration from VR gaming technology: Deep immersion and realistic interaction for scientific visualization. In *Proceedings of the 12th International Joint Conference on Computer Vision, Imaging and Computer Graphics Theory and Applications - Volume 3: IVAPP, VISIGRAPP* (2017), pp. 330–334. doi:10.5220/0006262903300334. 2

[Cab11] CABELLO R.: ThreeJS. https://threejs.org/, 2011. URL: https://threejs.org/. 4

[CC06] CLAYPOOL M., CLAYPOOL K.: Latency and player actions in online games. *Communications of the ACM 49*, 11 (Nov. 2006), 40–45. doi:10.1145/1167838.1167860. 4

[CC16] CHERUKURU, N. W., CALHOUN, R.: Augmented reality based doppler lidar data visualization: Promises and challenges. *EPJ Web of Conferences 119* (2016), 14006. doi:10.1051/epjconf/201611914006. 2

[CDD*09] COHEN J., DOLAN B., DUNLAP M., HELLERSTEIN J. M., WELTON C.: MAD skills: New analysis practices for big data. *Proceedings of the VLDB Endowment 2* (2009), 1481–1492. doi:10.14778/1687553.1687576. 1, 2

[CKB09] COCKBURN A., KARLSON A., BEDERSON B. B.: A review of overview+detail, zooming, and focus+context interfaces. *ACM Computing Surveys 41* (2009), 2:1–2:31. doi:10.1145/1456650.1456652. 4

[EHRF08] ELMQVIST N., HENRY N., RICHE Y., FEKETE J.-D.: Melange: Space folding for multi-focus interaction. In *Proceedings of the SIGCHI Conference on Human Factors in Computing Systems* (2008), CHI '08, ACM, pp. 1333–1342. doi:10.1145/1357054.1357263. 4

[FH09] FOX P., HENDLER J. A.: Semantic escience: encoding meaning in next-generation digitally enhanced science. *The Fourth Paradigm: Data-Intensive Scientific Discovery* (2009), 147–152. 1, 2

[HBF*15] HOFMEISTER P. G., BOLLIG C., FAYED S., KUNZE M., REUTER R.: A compact doppler wind lidar for controlling the operation of wind turbines. *EARSeL eProceedings 14*, 1 (2015), 1. 2

[HH05] HENDERSON S. W., HANNON S. M.: Advanced coherent lidar system for wind measurements. *Proc. SPIE 5887* (2005), 58870I. doi:10.1117/12.620318. 2

[HHO*96] HANKIN S., HARRISON D. E., OSBORNE J., DAVISON J., O'BRIEN K.: A strategy and a tool, Ferret, for closely integrated visualization and analysis. *The Journal of Visualization and Computer Animation 7* (1996), 149–157. doi:10.1002/(SICI)1099-1778(199607)7:3<149::AID-VIS148>3.0.CO;2-X. 2

[KAW*13] KALTHOFF N., ADLER B., WIESER A., KOHLER M., TRÄUMNER K., HANDWERKER J., CORSMEIER U., KHODAYAR S., LAMBERT D., KOPMANN A., KUNKA N., DICK G., RAMATSCHI M., WICKERT J., KOTTMEIER C.: KITcube – a mobile observation platform for convection studies deployed during HyMeX. *Meteorologische Zeitschrift 22*, 6 (2013), 633–647. doi:10.1127/0941-2948/2013/0542. 2

[KCC*15] KNIPPERTZ P., COE H., CHIU J. C., EVANS M. J., FINK A. H., KALTHOFF N., LIOUSSE C., MARI C., ALLAN R. P., BROOKS B., DANOUR S., FLAMANT C., JEGEDE O. O., LOHOU F., MARSHAM J. H.: The DACCIWA project: Dynamics–aerosol–chemistry–cloud interactions in West Africa. *Bulletin of the American Meteorological Society 96* (2015), 1451–1460. doi:10.1175/BAMS-D-14-00108.1. 2

[Khr11] KHRONOS: WebGL - OpenGL ES 2.0 for the Web, https://www.khronos.org/webgl/, 2011. URL: https://www.khronos.org/webgl/. 2

[LJH13] LIU Z., JIANG B., HEER J.: imMens: Real-time visual querying of big data. In *Proceedings of the 15th Eurographics Conference on Visualization* (2013), EuroVis '13, The Eurographs Association; John Wiley & Sons, Ltd., pp. 421–430. doi:10.1111/cgf.12129. 1, 3

[Mad12] MADDEN S.: From databases to big data. *IEEE Internet Computing 16*, 3 (2012), 4–6. doi:10.1109/MIC.2012.50. 1, 2

[MAT10] MATLAB: *version 7.10.0 (R2010a)*. The MathWorks Inc., Natick, Massachusetts, 2010. 2

[MKRE16] MWALONGO F., KRONE M., REINA G., ERTL T.: State-of-the-art report in web-based visualization. *Computer Graphics Forum 35* (2016), 553–575. doi:10.1111/cgf.12929. 4

[NSBW08] NOCKE T., STERZEL T., BÖTTINGER M., WROBEL M.: Visualization of climate and climate change data: An overview. *Digital earth summit on geoinformatics* (2008), 226–232. 1

[PSV*15] PRASAD N. S., SIBELL R., VETORINO S., HIGGINS R., TRACY A.: An all-fiber, modular, compact wind lidar for wind sensing and wake vortex applications. In *SPIE Defense and Security* (2015), International Society for Optics and Photonics, pp. 94650C–94650C. 2

[RTL*16] ROBERTS R. C., TONG C., LARAMEE R. S., SMITH G. A., BROOKES P., D'CRUZE T.: Interactive Analytical Treemaps for Visualisation of Call Centre Data. In *Smart Tools and Apps for Graphics - Eurographics Italian Chapter Conference* (2016), Pintore G., Stanco F., (Eds.), The Eurographics Association. doi:10.2312/stag.20161370. 4

[SFK13] SCHUSTER R., FINK A. H., KNIPPERTZ P.: Formation and maintenance of nocturnal low-level stratus over the southern west african monsoon region during amma 2006. *Journal of the Atmospheric Sciences 70*, 8 (2013), 2337–2355. doi:10.1175/JAS-D-12-0241.1. 1, 4

[SGK10] SHARMA R., GUPTA M., KAPOOR G.: Some better bounds on the variance with applications. *Journal of Mathematical Inequalities 4*, 3 (2010), 355–363. doi:dx.doi.org/10.7153/jmi-04-32. 4

[SN14] SCHNEIDER B., NOCKE T.: *Image Politics of Climate Change: Visualizations, Imaginations, Documentations*. Image (Bielefeld). Transcript Verlag, 2014. 1

[TDN11] TOMINSKI C., DONGES J. F., NOCKE T.: Information visualization in climate research. In *2011 15th International Conference on Information Visualisation* (2011), pp. 298–305. doi:10.1109/IV.2011.12. 1, 2

[TJCS*17] TAN JEROME N., CHILINGARYAN S., SHKARIN A., KOPMANN A., ZAPF M., LIZIN A., BERGMANN T.: WAVE: A 3D online previewing framework for big data archives. In *Proceedings of the 12th International Joint Conference on Computer Vision, Imaging and Computer Graphics Theory and Applications - Volume 3: IVAPP, VISIGRAPP* (2017), pp. 152–163. doi:10.5220/0006228101520163. 2, 3, 4

[TLCS12] THOBOIS L., LOAEC S., CARIOU J.-P., SAUVAGE L.: Measuring wake vortices and wind shears in real-time with a scanning wind doppler lidar. 92nd American Meteorological Society Annual Meeting, 2012. URL: https://ams.confex.com/ams/92Annual/webprogram/Paper199227.html. 2

[WHW13] WANG Y., HUYNH G., WILLIAMSON C.: Integration of google maps/earth with microscale meteorology models and data visualization. *Comput. Geosci. 61* (2013), 23–31. doi:10.1016/j.cageo.2013.07.016. 2

[ZCPB11] ZHAO J., CHEVALIER F., PIETRIGA E., BALAKRISHNAN R.: Exploratory analysis of time-series with chronolenses. *IEEE Transactions on Visualization and Computer Graphics 17* (2011), 2422–2431. doi:10.1109/TVCG.2011.195. 4